Journal of Engineering and Applied Sciences 13 (13): 4887-4891, 2018
ISSN: 1816-949X

Thermal Performance Characteristics of Three Sides 60° Inclined Wire Roughened Solar Air Heater

Ravi Kumar, L. Prasad and B.N. Prasad
Department of Mechanical Engineering, National Institute of Technology,
831014 Jamshedpur, India

Abstract: Three sides 60° wire roughened solar air heater together with on side 60° wire roughened solar air heater has been investigated. Effect of roughness and flow parameter, p/e, e/D and Re on thermal performance of the collectors has been represented. Three sides 60° wire roughened solar air heater has been found to be thermally more efficient by an amount of about 14-46% than that of one side roughened one in the range of parameters investigated.

key words: Artificial roughness, angle of attack, collector efficiency factor, collector heat removal factor, parameter, investigated

INTRODUCTION

The renewable energy sources playing a vital role to fulfil the required energy demand in industrialization and economical progress. Plenty of research works in the area of solar air heaters where enhancement of the efficiency of solar air heater by using different types of solar air heaters and various roughness elements and alignments are available in literature.

Generally thermal efficiency of solar air heaters is poor due to low convective heat transfer coefficient between the absorber plate and air flowing through the flow duct. The reason behind this is the formation of laminar viscous sub layer, adjacent to the wall which resists heat transfer. Thus, to enhance the heat transfer, provision of artificial roughness on the flow sides of solar air heater is introduced.

Use of artificial roughness on heat transferring surface creates artificial turbulency in the viscosity of the wall. Artificially roughened solar air heater is considered better to increase the heat transfer coefficient, since, artificial roughness elements break the laminar-sub-layer and reduce the thermal resistance. But simultaneously it increases the frictional losses in solar duct. Therefore, the requirement of turbulence to be created using artificial roughness should remain in the region very close to the heat transferring surface, i.e. within the laminar-sub-layer thickness only to reduce the friction loss. This can be possible by using the height of roughness elements to be small in comparison with the duct dimension (Patil *et al*., 2012), limited to the laminar-sub-layer thickness of hydrodynamic boundary layer (Prasad and Saini,1991).

Roughness geometries have been classified in four categories for solar air heater (Bhushan and Singh, 2011). Heat transfer and friction factor in artificially roughened solar air heater duct having these four types of roughness geometries have been found experimentally by various researchers (Prasad and Saini, 1988; Gupta *et al*., 1993; Saini and Saini, 1997; Jaurkar *et al*., 2006; Karmare and Tikekar, 2007; Singh *et al*., 2011; Lanjewar *et al*., 2011; Bhusan and Singh, 2011). Also, the thermal performance and heat transfer coefficient were reported by Chamoli *et al*. (2012a, b), Gawande *et al*. (2014), Saurav and Bartaria (2013), Shakya *et al*. (2013), Saini *et al*. (2007), Yadav and Bhagoria (2013, 2014a, b), Chabane *et al*. (2014), Prasad *et al*. (2015) and Adeyemo and Adeoye (2008). Nusselt number and friction factor correlations were developed by using these experimental data. The thermal performance in double flow solar air heater with aluminium cans has been investigated by (Ozgen *et al*., 2009). But all these works remained limited to only one top side artificial roughness. Recently the research has been extended and experimentally investigated in three sides roughened solar air heaters, i.e., roughness used in top side as well as both side walls (Prasad *et al*., 2014, 2015; Behura *et al*., 2016). It has been found that the three sides roughened solar air heater is more effective and efficient than the one side roughened solar air heater. The roughness has been also used at different angle of attack and 60° angle of attack has been found most effective to enhance the thermal performance of only top side roughened solar air heaters by Behura *et al*. (2016). This study reports the results of

Corresponding Author: Ravi Kumar, Department of Mechanical Engineering, National Institute of Technology, 831014 Jamshedpur, India

experimentally collected data in actual outdoor conditions on thermal performance of three sides 60° inclined wire roughened solar air heaters.

MATERIALS AND METHODS

Investigation: Figure 1 shows the schematic diagram of a typical three sides artificially roughened solar air heater duct model having three sides covered by glass. The duct height is 25 mm and the width is 200 mm, the glass covers are 4 mm thick ordinary glass. The absorber plates are galvanised-iron sheets of 20 standard wire gauge. Fluid temperature measured by digital thermometer of least count 0.1°C and the plate temperatures were measured by the thermocouples of 28 standard wire gauge. Pyranometer is used to measure the solar radiations. The pressure drop is measured along the test study by the help of the multi tube manometer.

The roughness element height is selected using the equations under used in (Prasad and Saini,1991) because the roughness height should fall within the laminar sub-layer thickness of hydrodynamic boundary layer and it won't protrude beyond it:

$$\frac{\partial'}{D}=\frac{58}{Re^{\frac{7}{8}}} \quad (1)$$

$$\frac{\partial'}{D}=\frac{140.185}{Re} \quad (2)$$

The data were collected simultaneously on both three sides and one side roughened solar air heaters. The experimental values of the heat transfer coefficient for the both one side and three side 60^0 inclined wire roughened solar air heaters have been found by Eq. 3 as given:

$$C_p(t_0-t_i)=hA_c(\overline{t_p}-t_f) \quad (3)$$

Which may be further used to obtain the values of Nusselt number for the both solar air heaters by Eq. (4) under:

$$Nu=\frac{hD}{k} \quad (4)$$

Artificial roughness have been provided on the fluid flow side of the absorber plate normal to the fluid flow direction at varying values of relative roughness pitch,p/e in the range of 10-20, relative roughness height, e/D in the range of 0.0180-0.0248. Flow Reynolds number, Re, varied in between 2000-16000 and angle of attack, α is 60°.

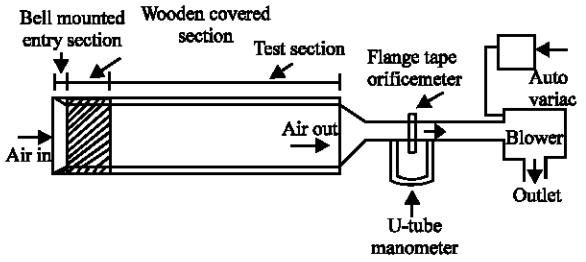

Fig. 1: Schematic diagram of three sides artificial roughened and glass covered solar air heater

RESULTS AND DISCUSSION

Thermal performance has been represented on the basis of outlet air temperature for solar air heaters, operating without recycling of air (Gupta *et al*., 1997). Equation 5 has formed the basis of representation of thermal efficiency:

$$\left(th=F_R(\tau\alpha)-F_RU_L(t_0-t_\alpha)\right)/I \quad (5)$$

This could be written as Eq. 6 based on fluid outlet temperature:

$$\left(th=F_o(\tau\alpha)-F_oU_L(t_o-t_\alpha)\right)/I \quad (6)$$

For inlet temperature, t_i, to be the same as ambient temperature, t_α, Eq. 6 takes the form as of Eq. 7 under:

$$\left(th=F_o(\tau\alpha)-F_oU_L(t_o-t_i)\right)/I \quad (7)$$

And the instantaneous thermal efficiency given by Eq. 8:

$$\left(th=\dot{m}C_p(t_o-t_i)\right)/I \quad (8)$$

Mass flow rate is the strong function which is highly recommended in order to obtain reasonably reliable information with regard to the thermal performance of solar air heaters. Each mass flow rate results in an efficiency curve (Gupta and Garg, 1967; ASHARE Standards, 1977; Reddy *et al*., 1980; Biondi *et al*., 1988). Fig. 2 shows the typical performance characteristics of one side andthree sides 60° inclined wire roughened solar air heaters at various mass flow rates and for the values of p/e, equal to 10 and e/D, equal to 0.0248.

The lines $\dot{m}_1$ - $\dot{m}_5$ shown in Fig. 1 are the efficiency curves for each mass flow rate based on Eq. 8. The upper points on these curves correspond to the three sides 60° inclined wire roughened collectors and the

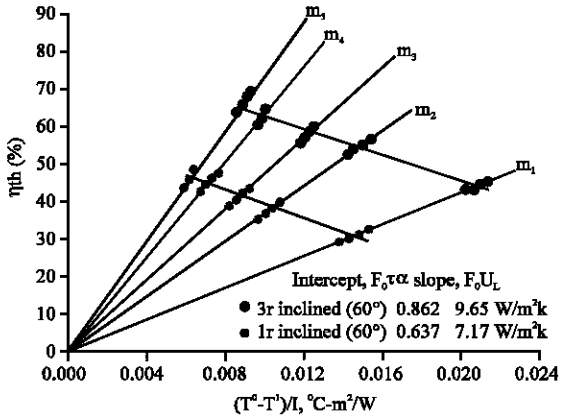

Fig. 2: Performance characteristic of solar air heaters

lower ones correspond to one side 60° inclined wire roughened collectors. The respective values of the intercept and slope have been found out and shown in this Fig. 1.

The values of the thermal performance parameters, F_R, and F' have been worked out by utilizing the following Eq. 9-11, written under (Bernier and Plett, 1988):

$$F_R(\tau\alpha) = F_o(\tau\alpha)\left[\frac{\dot{m}C_p / A_c}{\dot{m}C_p / A_c + F_oU_L}\right] \quad (9)$$

$$F_RU_L = F_oU_L\left[\frac{\dot{m}C_p / A_c}{\dot{m}C_p / A_c + F_oU_L}\right] \quad (10)$$

$$F' = GC_p\left[\ln\left(\frac{F_oU_L}{F_RU_L}\right)/U_L\right] \quad (11)$$

The respective values of the collector performance parameters $F_R$and F' have been plotted in Fig. 3-6 to see the effect of the roughness and flow parameters on $F_R$and F' in three sides and one side 60° inclined roughened solar air heaters. It could be seen from these Fig. 3-6 that the values of both the parameters F_R and F' is higher for three sides 60° inclined wire roughened solar air heater than those of one side 60° inclined wire roughened solar air heater by an amount in the range of 14-46%. It could also be attributed from these figures that the rate of increase in the values of $F_R$and F' is more at higher mass flow rates. As also, increasing value of the roughness parameter, p/e, results in decreasing values of both F_r and F' whereas increasing values of the roughness parameter, e/D, results in increasing values of both F_R and F'.

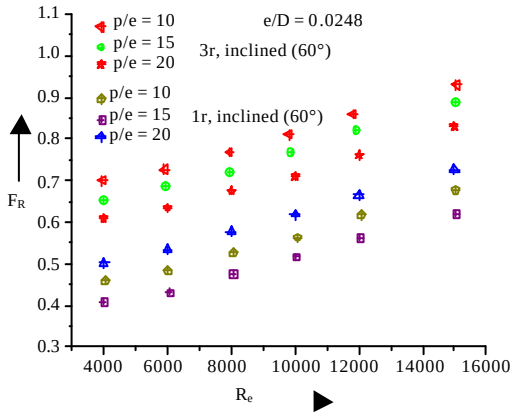

Fig. 3: Effect of p/e on collector heat removal factor in solar air heaters

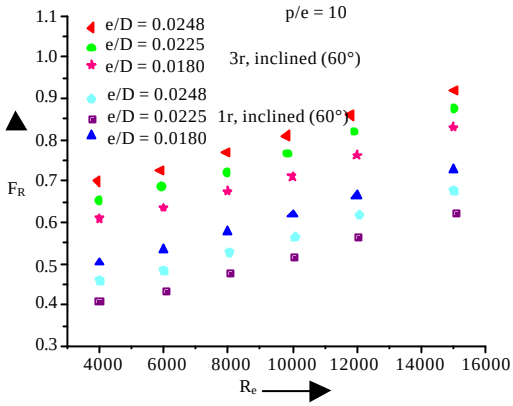

Fig. 4: Effect of e/D on collector heat removal factor in solar air heaters

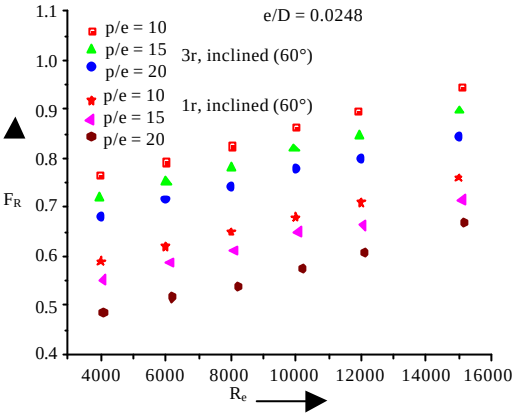

Fig. 5: Effect of p/e on collector efficiency factor in solar air heaters

Which further have been used to give the values of $F_R(\tau\alpha)$ and $F_RU_L$with the values obtained for the collector performance parameter $F_R(\tau\alpha)$ and F_RU_L for the respective solar air heaters and based on the conventional thermal

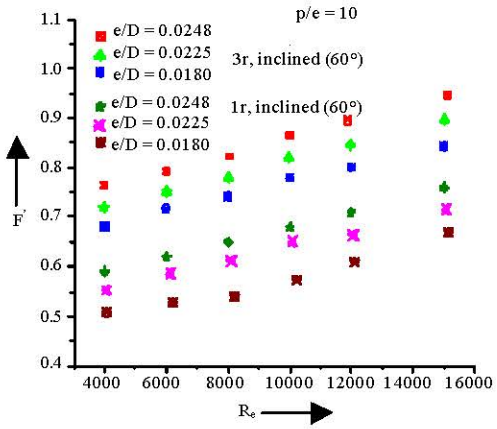

Fig. 6: Effect of e/D on collector efficiency factor in solar air heaters

performance equations the following thermal performance Eq. 12 and 13, for the respective solar air heaters have been obtained as under:

$$\eta_{th}(3r, \text{inclined}) = 0.892(\tau\alpha) - \left[0.892U_L\left(\frac{t_i - t_a}{I}\right)\right] \quad (12)$$

$$\eta_{th}(1r, \text{inclined}) = 0.678(\tau\alpha) - \left[0.678U_L\left(\frac{t_i - t_a}{I}\right)\right] \quad (13)$$

CONCLUSION

Three sides 60° inclined wire roughened solar air heater perform better than one side 60° inclined wire roughened solar air heater under the same operating conditions of roughness and flow parameters.

The values of the heat removal factor, F_R and plate efficiency factor, F' have been found to increase in the range of 14-46% over than of one side 60° wire roughened solar air heaters. The conventional thermal performance equations for three sides 60° wire roughened and one side 60° wire roughened solar air heaters have been derived as under:

$$\eta_{th}(3r, \text{inclined}) = 0.892(\tau\alpha) - \left[0.892U_L\left(\frac{t_i - t_a}{I}\right)\right] \quad (14)$$

$$\eta_{th}(1r, \text{inclined}) = 0.678(\tau\alpha) - \left[0.678U_L\left(\frac{t_i - t_a}{I}\right)\right] \quad (15)$$

NOMENCLATURE

A_c = Collector area (m^2)
C_p = Specific heat at constant pressure of air (kJ/kg K)
D = Hydraulic diameter of solar air heater duct (m)
e/D = Relative roughness height
F' = Collector efficiency factor
F_R = Collector heat removal factor
F_o = Collector heat removal factor based on outlet temperature (t_o)
G = Mass flow rate per unit collector area (kg/sm^2)
h = Convective heat transfer coefficient (W/m^2K)
I = Intensity of solar radiation (W/m^2)
k = Thermal conductivity of collector material (W/m K)
L = Collector Length (m)
l = Length of the test section (m)
$\dot{m}$ = Mass flow rate (kg/sec)
Nu = Nusselt number
p/e = relative roughness pitch
Re = Reynolds number
t_a = Ambient temperature (°C)
t_o = Outlet air temperature (°C)
t_i = Inlet air temperature (°C)
$\overline{t_p}$ = Average plate temperature (°C)
$\overline{t_f}$ = Average fluid temperature (°C)
U_L = Overall heat transfer coefficient (W/m^2 K)
α = Angle of attack, degrees
$\tau\alpha$ = Transmittance-absorptance product
ηth = Collector thermal efficiency
∂' = Laminar sub-layer thickness (m)

SUFFIX

1r = Top side inclined roughened solar air heater
3r = Three sides inclined roughened solar air heater

REFERENCES

ASHARE Standards, 1977. Methods of testing to determine the thermal performance of solar collectors. ASHARE Standards, Atlanta, Georgia.

Adeyemo, S.B. and O.F. Adeoye, 2008. Comparative performance of two discrete solar collectors. J. Eng. Appl. Sci., 3: 228-232.

Behura, A.K., B.N. Prasad and L. Prasad, 2016. Heat transfer, friction factor and thermal performance of three sides artificially roughened solar air heaters. Sol. Energy, 130: 46-59.

Bernier, M.A. and E.G. Plett, 1988. Thermal performance representation and testing of air solar collectors. J. Sol. Energy Eng., 110: 74-81.

Bhushan, B. and R. Singh, 2011. Nusselt number and friction factor correlations for solar air heater duct having artificially roughened absorber plate. Sol. Energy, 85: 1109-1118.

Biondi, P., L. Cicala and G. Farina, 1988. Performance analysis of solar air heaters of conventional design. Sol. Energy, 41: 101-107.

Chabane, F., N. Moummi and S. Benramache, 2014. Experimental study of heat transfer and thermal performance with longitudinal fins of solar air heater. J. Adv. Res., 5: 183-192.

Chamoli, S., N.S. Thakur and J.S. Saini, 2012a. A review of turbulence promoters used in solar thermal systems. Renewable Sustainable Energy Rev., 16: 3154-3175.

Chamoli, S., R. Chauhan, N.S. Thakur and J.S. Saini, 2012b. A review of the performance of double pass solar air heater. Renewable Sustainable Energy Rev., 16: 48-492.

Gawande, V.B., A.S. Dhoble and D.B. Zodpe, 2014. Effect of roughness geometries on heat transfer enhancement in solar thermal systems: A review. Renewable Sustainable Energy Rev., 32: 347-378.

Gupta, C.L. and H.P. Garg, 1967. Performance studies on solar air heaters. Sol. Energy, 11: 25-31.

Gupta, D., S.C. Solanki and J.S. Saini, 1993. Heat and fluid flow in rectangular solar air heater ducts having transverse rib roughness on absorber plates. Sol. Energy, 51: 31-37.

Gupta, D., S.C. Solanki and J.S. Saini, 1997. Thermohydraulic performance of solar air heaters with roughened absorber plates. Sol. Energy, 61: 33-42.

Jaurker, A.R., J.S. Saini and B.K. Gandhi, 2006. Heat transfer and friction characteristics of rectangular solar air heater duct using rib-grooved artificial roughness. Sol. Energy, 80: 895-907.

Karmare, S.V. and A.N. Tikekar, 2007. Heat transfer and friction factor correlation for artificially roughened duct with metal grit ribs. Intl. J. Heat Mass Transfer, 50: 4342-4351.

Lanjewar, A., J.L. Bhagoria and R.M. Sarviya, 2011. Heat transfer and friction in solar air heater duct with W-shaped rib roughness on absorber plate. Energy, 36: 4531-4541.

Ozgen, F., M. Esen and H. Esen, 2009. Experimental investigation of thermal performance of a double-flow solar air heater having Aluminium cans. Renewable Energy, 34: 2391-2398.

Patil, A.K., J.S. Saini and K. Kumar, 2012. A comprehensive review on roughness geometries and investigation techniques used in artificially roughened solar air heaters. Intl. J. Renewable Energy Res., 2: 1-15.

Prasad, B.N. and J.S. Saini, 1991. Optimal thermohydraulic performance of artificially roughened solar air heaters. Sol. Energy, 47: 91-96.

Prasad, B.N., A. Kumar and K.D.P. Singh, 2015. Optimization of thermo hydraulic performance in three sides artificially roughened solar air heaters. Sol. Energy, 111: 313-319.

Prasad, B.N., A.K. Behura and L. Prasad, 2014. Fluid flow and heat transfer analysis for heat transfer enhancement in three sided artificially roughened solar air heater. Sol. Energy, 105: 27-35.

Prasad, B.N.and J.S. Saini, 1988. Effect of artificial roughness on heat transfer and friction factor in a solar air heater. Sol. Energy, 41: 555-560.

Reddy, T.A. and C.L. Gupta, 1980. Generating application design data for solar air heating systems. Sol. Energy, 25: 527-530.

Saini, R.P. and J.S. Saini, 1997. Heat transfer and friction factor correlations for artificially roughened ducts with expanded metal mesh as roughness element. Intl. J. Heat Mass Transfer, 40: 973-986.

Saini, R.P. and S.K. Singal, 2007. A review on roughness geometry used in solar air heaters. Sol. Energy, 81: 1340-1350.

Saurav, S. and V.N. Bartaria, 2013. Heat transfer and thermal efficiency of solar air heater having artificial roughness: A review. Intl. J. Renewable Energy Res., 3: 498-508.

Shakya, U., R.P. Saini and M.K. Singhal, 2013. A review on artificial roughness geometry for enhancement of heat transfer and friction characteristic on roughened duct of solar air heater. Intl. J. Emerg. Technol. Adv. Eng., 3: 279-287.

Singh, S., S. Chander and J.S. Saini, 2011. Heat transfer and friction factor correlations of solar air heater ducts artificially roughened with discrete V-down ribs. Energy, 36: 5053-5064.

Yadav, A.S. and J.L. Bhagoria, 2013. A CFD (Computational Fluid Dynamics) based heat transfer and fluid flow analysis of a solar air heater provided with circular transverse wire rib roughness on the absorber plate. Energy, 55: 1127-1142.

Yadav, A.S. and J.L. Bhagoria, 2014b. A CFD based thermo-hydraulic performance analysis of an artificially roughened solar air heater having equilateral triangular sectioned rib roughness on the absorber plate. Intl. J. Heat Mass Transfer, 70: 1016-1039.

Yadav, A.S. and J.L. Bhagoria, 2014a. A numerical investigation of square sectioned transverse rib roughened solar air heater. Intl. J. Thermal Sci., 79: 111-131.